

# Journal of Biomedical Optics

SPIEDigitalLibrary.org/jbo

## **Spiking cortical model–based nonlocal means method for speckle reduction in optical coherence tomography images**

Xuming Zhang  
Liu Li  
Fei Zhu  
Wenguang Hou  
Xinjian Chen



# Spiking cortical model–based nonlocal means method for speckle reduction in optical coherence tomography images

Xuming Zhang,<sup>a</sup> Liu Li,<sup>a</sup> Fei Zhu,<sup>a</sup> Wenguang Hou,<sup>a,\*</sup> and Xinjian Chen<sup>b</sup>

<sup>a</sup>Huazhong University of Science and Technology, School of Life Science and Technology, 1037 Luoyu Road, Wuhan 430074, China

<sup>b</sup>Soochow University, School of Electronics and Information, 1 Shizi Street, Suzhou 215006, China

**Abstract.** Optical coherence tomography (OCT) images are usually degraded by significant speckle noise, which will strongly hamper their quantitative analysis. However, speckle noise reduction in OCT images is particularly challenging because of the difficulty in differentiating between noise and the information components of the speckle pattern. To address this problem, the spiking cortical model (SCM)-based nonlocal means method is presented. The proposed method explores self-similarities of OCT images based on rotation-invariant features of image patches extracted by SCM and then restores the speckled images by averaging the similar patches. This method can provide sufficient speckle reduction while preserving image details very well due to its effectiveness in finding reliable similar patches under high speckle noise contamination. When applied to the retinal OCT image, this method provides signal-to-noise ratio improvements of >16 dB with a small 5.4% loss of similarity. © 2014 Society of Photo-Optical Instrumentation Engineers (SPIE) [DOI: 10.1117/1.JBO.19.6.066005]

Keywords: optical coherence tomography; speckle reduction; nonlocal means; spiking cortical model.

Paper 140198LR received Mar. 26, 2014; revised manuscript received May 8, 2014; accepted for publication May 12, 2014; published online Jun. 11, 2014.

Optical coherence tomography (OCT) is a kind of noninvasive high-resolution biomedical imaging technology based on low coherence interferometry. The principle behind OCT imaging leads to presence of speckle in the OCT images. Because speckle carries both a noise component and structural information about the imaged object, it is very challenging to suppress speckle noise effectively. Various algorithms have been proposed to despeckle OCT images. The two classes of state-of-the-art despeckling methods are wavelet-, curvelet-, or contourlet-based methods<sup>1-4</sup> and anisotropic diffusion-based methods.<sup>5,6</sup> These methods tend to provide limited speckle noise suppression or reduce the sharpness of structural details in the case of high speckle noise corruption.

Recently, a nonlocal means (NLM) method<sup>7</sup> has been proposed, which explores image self-similarities by the nonlocal comparison of image patches for image denoising. The NLM method, originally designed for Gaussian noise removal, has lately been applied to remove speckle noise from ultrasound images<sup>8</sup> and synthetic aperture radar images.<sup>9</sup> This paper aims to extend this method to restore OCT images. However, the NLM method measures the similarity between pixels based on the intensities of image patches only in the translational sense without considering the orientation of each patch. Therefore, it is difficult for this method to preserve intricate details of speckled OCT images involving rotated similar patterns. To address this problem, the spiking cortical model (SCM) proposed in Ref. 10 is introduced into the NLM method to despeckle OCT images by exploring rotation-invariant self-similarities of speckled images.

Derived from several other visual cortices, the SCM is a laterally connected two-dimensional neural network. When the SCM is used for image processing, each network neuron corresponds to an input image pixel. The neuron  $N_{i,j}$  at  $(i, j)$  in the SCM receives the corresponding pixel's normalized intensity  $T_{i,j}$  as an external stimulus and receives local stimuli from its neighboring neurons. When the combined external and local stimuli  $F_{i,j}$ , the internal activity, exceeds a dynamic threshold  $\Theta_{i,j}$ ,  $N_{i,j}$  will fire and generate a pulse output  $Y_{i,j}$ . In the  $n$ 'th iteration, these variables are computed as<sup>10</sup>

$$F_{i,j}[n] = fF_{i,j}[n-1] + T_{i,j} + T_{i,j} \sum_{k,l} W_{i,j,k,l} Y_{k,l}[n-1], \quad (1)$$

$$\Theta_{i,j}[n] = g\Theta_{i,j}[n-1] + hY_{i,j}[n-1], \quad (2)$$

$$Y_{i,j}[n] = \begin{cases} 1, & F_{i,j}[n] > \Theta_{i,j}[n] \\ 0, & F_{i,j}[n] \leq \Theta_{i,j}[n] \end{cases}, \quad (3)$$

where  $f$  and  $g$  are constants  $<1$  and  $h$  is a large constant for adjustment of the threshold magnitude;  $W_{i,j,k,l}$  is the connection weight between the neuron  $N_{i,j}$  and its linking neuron  $N_{k,l}$ , and it is defined as  $W_{i,j,k,l} = [1/\sqrt{(i-k)^2 + (j-l)^2}]$  if  $(i, j) \neq (k, l)$  or otherwise  $W_{i,j,k,l} = 0$ . Equation (1) means that the pulse output of a neuron modulates the activity of its neighbors via the connection weight. Equation (2) shows that the pulse output of  $N_{i,j}$  will be fed back to modulate its dynamic threshold. Based on iterative computations, the SCM will produce a series of binary pulse images by Eq. (3). Since pulse images contain information of an input image, they can be used for feature

\*Address all correspondence to: Wenguang Hou, E-mail: [wenguanghou@gmail.com](mailto:wenguanghou@gmail.com)

generation. The entropy of pulse outputs has been utilized for image feature extraction.<sup>10</sup> Because the Tsallis entropy is suitable for measuring the information contained in the neurons,<sup>11</sup> it is computed for pulse images to extract the features from image patches in  $I$  in this paper.

Let  $U_{i,j}[n]$  be the  $L_w \times L_w$  similarity window centered at  $(i, j)$  in  $Y[n]$ . The probabilities  $P_{i,j}^1[n]$  and  $P_{i,j}^0[n]$  of 1's and 0's in  $U_{i,j}[n]$  are computed as the ratio of the number of firing pixels and that of nonfiring ones to the sum of pixels in  $U_{i,j}[n]$ , respectively. The Tsallis entropy is calculated by  $H(U_{i,j}[n]) = (1/\alpha - 1)\{1 - \sum_{k=0}^1 (P_{i,j}^k[n])^\alpha\}$ , where  $\alpha$  is an adjustable parameter chosen as  $\alpha = 2$  according to Ref. 11. The Tsallis entropy from the various iterations will form the feature vector  $V_{i,j}$  of the image patch centered at  $(i, j)$  in  $I$ , i.e.,  $V_{i,j} = \{H(U_{i,j}[1]), H(U_{i,j}[2]), \dots, H(U_{i,j}[n_{\max}])\}$ , where  $n_{\max}$  denotes the maximum iteration times. For two rotated repetitive patterns in  $I$ , their pulse images generated by the SCM will have the same number of firing pixels at each iteration, thereby leading to the same Tsallis entropy. It follows that  $V$  is rotation-invariant. By introducing  $V$  into the comparison of image patches, the SCM-based NLM (SNLM) method can represent rotation-invariant self-similarities of OCT images effectively. Accordingly, the similarity  $S_{i,j,p,q}$  between two pixels at  $(i, j)$  and  $(p, q)$  in  $I$  is defined as

$$S_{i,j,p,q} = \begin{cases} \left(1 - \frac{\|V_{i,j} - V_{p,q}\|_2^2}{d^2}\right)^{1/8}, & \|V_{i,j} - V_{p,q}\|_2 \leq d, \\ 0, & \|V_{i,j} - V_{p,q}\|_2 > d \end{cases}, \quad (4)$$

where  $d$  denotes the decay parameter and  $\|\cdot\|_2$  is the Euclidean norm. In Eq. (4), the pixel similarity is defined as a piecewise function in order to ensure good image restoration performance by dismissing highly dissimilar image patches from the similarity computation.

Based on  $S_{i,j,p,q}$ , the denoised intensity  $D_{i,j}$  of the pixel at  $(i, j)$  in  $I$  is defined as

$$D_{i,j} = \frac{\sum_{(p,q) \in \Omega_{i,j}} S_{i,j,p,q} I_{p,q}}{\sum_{(p,q) \in \Omega_{i,j}} S_{i,j,p,q}}, \quad (5)$$

where  $\Omega_{i,j}$  means the  $L_s \times L_s$  search window centered at  $(i, j)$  in  $I$ .

To verify the advantage of the SNLM method in determining image self-similarities over the NLM method, simulations have been done on the synthetical noise-free image [Fig. 1(a)] and the corresponding speckled image [Fig. 1(d)]. The weight denoting the similarity between the center pixel in the red box and other pixels in each of the two images is computed for the two compared methods using the  $5 \times 5$  similarity window. The distribution of weights is shown in Figs. 1(b), 1(c), 1(e), and 1(f). It is shown that the NLM method can find only the pixels with neighborhoods similar to the center pixel up to translation. However, the SNLM method can identify the pixels whose neighborhoods are similar to that of the center pixel up to both translation and rotation with good robustness to noise. The above comparison indicates that the SNLM method can represent self-similarities of speckled images more effectively than the NLM method.

To demonstrate the superiority of the SNLM method in denoising OCT images, the NLM method and the modified

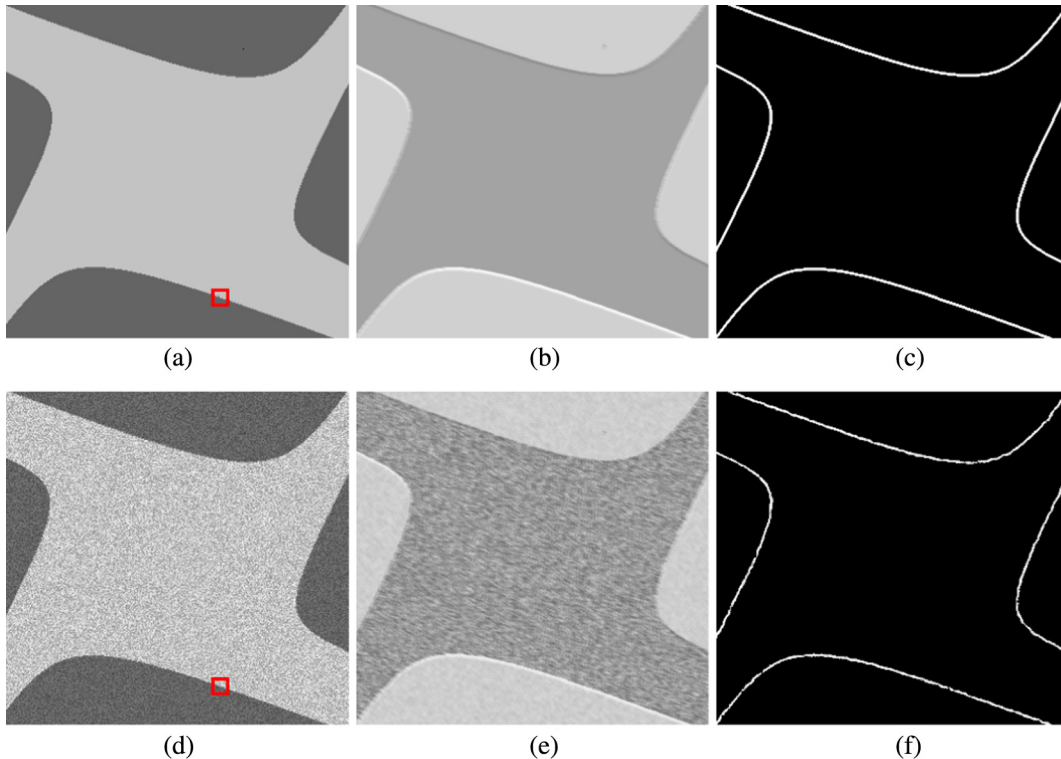


**Fig. 1** (a) and (d) The simulated noise-free image and the speckle-corrupted image, respectively. (b) and (e) The distribution of weights for the nonlocal means (NLM) method operating on (a) and (d), respectively. (c) and (f) The distribution of weights for the spiking cortical model (SCM)-based NLM (SNLM) method operating on (a) and (d), respectively.

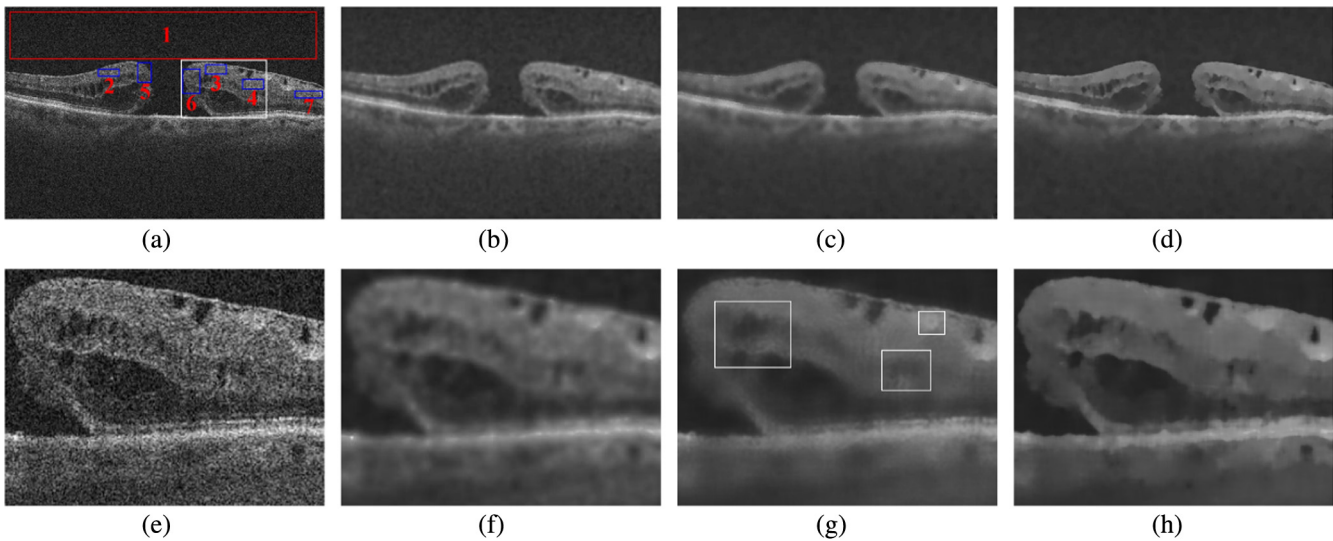


**Fig. 2** (a) to (d) The retinal optical coherence tomography (OCT) image, the images despeckled by the modified nonlinear complex diffusion filter (MNCDF), the NLM method, and the SNLM method, respectively. (e) to (h) The enlarged views of the region of interest for the original image and images despeckled by the MNCDF, the NLM method, and the SNLM method, respectively.

nonlinear complex diffusion filter (MNCDF)<sup>6</sup> have been used for comparisons. Experiments have been done on the three retinal OCT images [Figs. 2(a), 3(a), and 3(e)] of size  $924 \times 614$  pixels corresponding to  $6 \times 2$  mm. These images have been acquired using Cirrus HD-OCT system model 4000. In the experiments, the parameters in the MNCDF are chosen as suggested in Ref. 6. The SNLM method is insensitive to SCM parameters, and thus, we fix  $f = 0.8$ ,  $g = 0.7$ ,  $h = 80$ , and  $n_{\max} = 16$ . Meanwhile, we have chosen the  $7 \times 7$  similarity window ( $L_w = 7$ ) and the  $21 \times 21$  search window ( $L_s = 21$ ) for the NLM and SNLM methods while tuning the decay parameter in the two methods to obtain good restoration results.

The quantitative comparisons of restoration performance are made among the three despeckling methods operating on Fig. 2(a) acquired from the patient with macular hole. Because the noise-free OCT image is unknown, four quality

metrics are chosen for evaluating restoration performance, i.e., signal-to-noise ratio (SNR), average contrast-to-noise ratio (CNR),<sup>1</sup> average equivalent number of looks (ENL),<sup>1</sup> and cross-correlation (XCOR).<sup>3</sup> Both the SNR and CNR are computed using log scale data, while the ENL and XCOR are calculated using linear scale data. Table 1 lists the four metrics for the retinal OCT image, the images restored by the MNCDF, the NLM method with the decay parameter chosen as 70, and the SNLM method using  $d = 0.35 - 0.60$  with an interval of 0.05. Here, the SNR is computed on the background region (the box labeled 1). The CNR is averaged over the six regions (boxes labeled 2 to 7). The ENL is averaged over the three homogeneous regions (boxes labeled 2 to 4). We can see from Table 1 that the trade-off between speckle attenuation and similarity degradation is controlled by a single parameter  $d$ . In general, the increasing  $d$  will lead to improved speckle

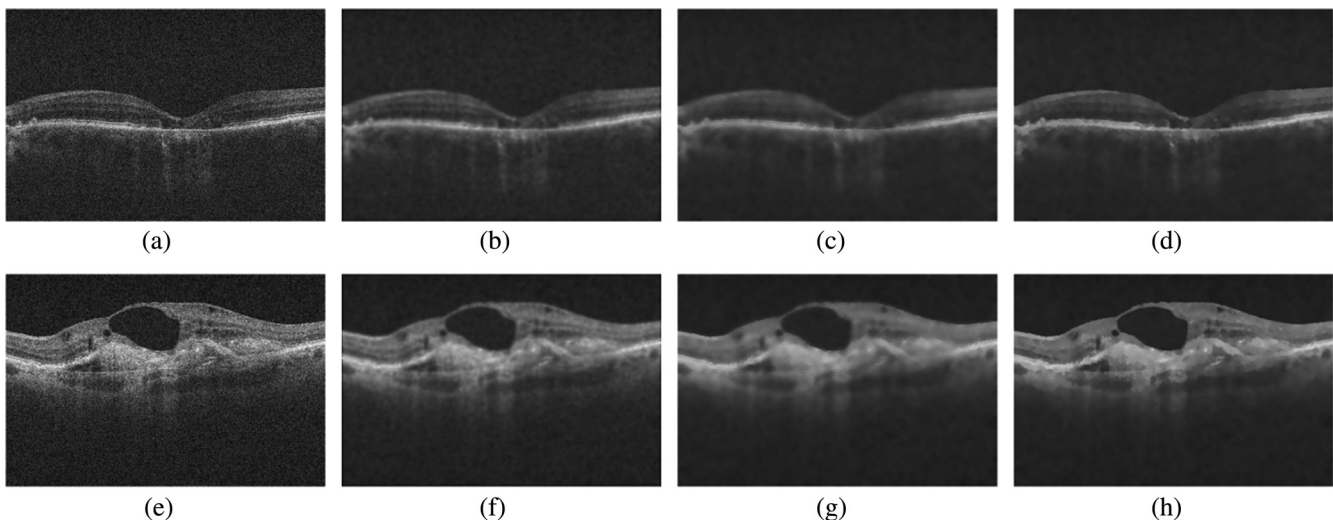


**Fig. 3** (a) and (e) The retinal OCT images. (b) to (d) Despeckled results for the MNCDF, the NLM method, and the SNLM method operating on (a), respectively. (f) to (h) Despeckled results for the MNCDF, the NLM method, and the SNLM method operating on (e), respectively.

**Table 1** Image quality metrics.

Image	SNR (dB)	CNR (dB)	ENL	XCOR
Original NLM MNCDF	24.31	2.29	12.36	1
	39.30	9.24	475.33	0.944
	39.17	8.27	265.38	0.944
SNLM, $d = 0.35$	40.85	9.03	430.68	0.947
SNLM, $d = 0.40$	40.96	9.49	579.69	0.946
SNLM, $d = 0.45$	40.81	9.82	738.68	0.946
SNLM, $d = 0.50$	40.44	10.02	873.61	0.944
SNLM, $d = 0.55$	40.07	10.13	970.42	0.943
SNLM, $d = 0.60$	39.60	10.14	988.93	0.942

Note: SNR, signal-to-noise ratio; CNR, contrast-to-noise ratio; ENL, equivalent number of looks; XCOR, cross-correlation; NLM, nonlocal means; MNCDF, modified nonlinear complex diffusion filter; SNLM, spiking cortical model-based NLM.

reduction performance, but poorer detail preservation performance. Based on the comprehensive consideration of four metrics, we have chosen  $d = 0.45$  for despeckling the OCT image. Table 1 shows that the SNLM method using  $d = 0.45$  provides significant SNR, CNR, and ENL improvements over other methods. Compared with the original image, the SNLM method improves the SNR by 16.5 dB, the CNR by 7.53 dB, and the ENL by a factor of  $\sim 60$  times with a small similarity reduction of 5.4%. Meanwhile, the proposed method outperforms the NLM method by providing slightly higher XCOR as well as SNR, CNR, and ENL improvements by 1.51 dB, 0.58 dB, and 1.55 times, respectively.

Figure 2 shows the retinal OCT image, the restored images, the enlarged views of the region of interest marked with the white box, and the corresponding regions despeckled by the three compared methods. We can see from Fig. 2 that the MNCDF cannot deliver sufficient speckle suppression and causes blurring of image details due to oversmoothing. The NLM method can suppress speckle noise effectively, but it damages some important image details as indicated by three white boxes in Fig. 2(g). By comparison, the SNLM method provides effective speckle reduction in the background region dominated by speckle noise as well as other regions where noise is superimposed on the signals. Furthermore, comparisons of the enlarged views further demonstrate that the SNLM method not only maintains the edge sharpness of the original signals very well, but also significantly improves the contrast and the visibility of image features, which will facilitate quantitative analysis of OCT images. To demonstrate the generalization of

the SNLM method, Fig. 3 shows the restoration results for three despeckling methods operating on other two OCT images. Likewise, the visual comparisons show that the proposed method performs significantly better than the two compared methods in terms of speckle reduction and edge preservation.

As regards the computational efficiency of the SNLM method, its mean runtime for three OCT images is  $\sim 13$  s, nearly four times that of the NLM method, when implemented using Visual C++6.0 on an Intel Dual Core 2.4-GHz processor with 4.0 GB of RAM.

In conclusion, the SNLM method provides a novel means for reducing speckle noise in OCT images by exploring rotation-invariant self-similarities of noisy images with good noise immunity. Experimentally, it has been shown that the SNLM method can restore OCT images effectively in terms of both objective criteria (SNR, CNR, ENL, and XCOR) and subjective human vision. We anticipate that this method can be utilized in a wide range of medical fields, such as ophthalmology, dermatology, gastroenterology, dentistry, and intraarterial imaging.

### Acknowledgments

The authors are grateful to Professor Andrzej Zajac and Professor Jan Kasprzak from Medical University of Warsaw for providing retinal optical coherence tomography images. This work is supported by the Project of the National 12th-Five Year Research Program of China (Grant No. 2012BAI13B02).

### References

1. D. C. Adler, T. H. Ko, and J. G. Fujimoto, "Speckle reduction in optical coherence tomography images by use of a spatially adaptive wavelet filter," *Opt. Lett.* **29**(24), 2878–2880 (2004).
2. J. Xu et al., "Wavelet domain compounding for speckle reduction in optical coherence tomography," *J. Biomed. Opt.* **18**(9), 096002 (2013).
3. Z. Jian et al., "Speckle attenuation in optical coherence tomography by curvelet shrinkage," *Opt. Lett.* **34**(10), 1516–1518 (2009).
4. J. Xu et al., "Speckle reduction of retinal optical coherence tomography based on contourlet shrinkage," *Opt. Lett.* **38**(15), 2900–2903 (2013).
5. P. Puvanathan and K. Bizheva, "Interval type-II fuzzy anisotropic diffusion algorithm for speckle noise reduction in optical coherence tomography images," *Opt. Express* **17**(2), 733–746 (2009).
6. R. Bernardes et al., "Improved adaptive complex diffusion despeckling filter," *Opt. Express* **18**(23), 24048–24059 (2010).
7. A. Buades, B. Coll, and J. M. Morel, "A review of image denoising algorithms, with a new one," *Multi. Model. Simul.* **4**(2), 490–530 (2005).
8. P. Coupé et al., "Nonlocal means-based speckle filtering for ultrasound images," *IEEE Trans. Image Process.* **18**(10), 2221–2229 (2009).
9. L. Torres et al., "Speckle reduction in polarimetric SAR imagery with stochastic distances and nonlocal means," *Pattern Recognit.* **47**(1), 141–157 (2014).
10. K. Zhan, H. Zhang, and Y. Ma, "New spiking cortical model for invariant texture retrieval and image processing," *IEEE Trans. Neural Netw.* **20**(12), 1980–1986 (2009).
11. R. Sneddon, "The Tsallis entropy of natural information," *Phys. A* **386**(1), 101–118 (2007).